Mechanisms underlying cortical activity during value-guided choice

Laurence T Hunt[1,2,*], **Nils Kolling**[1], **Alireza Soltani**[3], **Mark W Woolrich**[2,4], **Matthew FS Rushworth**[1,2], and **Timothy EJ Behrens**[2,5]

[1]Department of Experimental Psychology, University of Oxford, South Parks Road, Oxford OX1 3UD

[2]FMRIB Centre, University of Oxford, John Radcliffe Hospital, Oxford OX3 9DU

[3]Howard Hughes Medical Institute and Department of Neurobiology, Stanford University School of Medicine, Stanford, CA 94305

[4]Oxford Centre for Human Brain Activity (OHBA), University Department of Psychiatry, Warneford Hospital, Oxford OX3 7JX

[5]Wellcome Trust Centre for Neuroimaging, University College London, 12 Queen Square, London WC1N 3BG

Abstract

When choosing between two options, correlates of their value are represented in neural activity throughout the brain. Whether these representations reflect activity fundamental to the computational process of value comparison, as opposed to other computations covarying with value, is unknown. Here, we investigated activity in a biophysically plausible network model that transforms inputs relating to value into categorical choices. A set of characteristic time-varying signals emerged that reflect value comparison. We tested these model predictions in magnetoencephalography data recorded from human subjects performing value-guided decisions. Parietal and prefrontal signals matched closely with model predictions. These results provide a mechanistic explanation of neural signals recorded during value-guided choice, and a means of distinguishing computational roles of different cortical regions whose activity covaries with value.

Deciding upon the best course of action amongst a range of competing alternatives has been a fundamental problem addressed within the fields of economics[1], psychology[2], behavioural ecology[3], machine learning[4], and more recently, cognitive neuroscience[5-8]. To select the choice yielding greatest long-term reward, it has been proposed that neural circuits should take inputs reflecting the subjective value of alternatives, and compare these inputs to form a categorical decision[8]. Representations of value have been found in many cortical and subcortical brain regions[9-18] but whether and how activity changes in these representations might constitute the decision process itself is unknown. The uncertainty is partly a

consequence of not knowing how the signature of a decision would manifest itself at the level of the activity that can be recorded in a population of neurons.

One potential neuronal mechanism for value comparison is *competition by mutual inhibition*[19,20]. In this class of models, separate pools of neurons representing different options are excited by the value of their respective options, but inhibit each other such that activity only survives in the eventual winning pool. This mechanism is particularly attractive as it can be implemented in networks of neurons that respect known neurobiology[20]. Indeed, such models accurately predict single cell activity in the parietal cortex during *perceptual* decisions[21].

It has been proposed that similar mechanisms might also underlie value-guided choice, but this proposal has rarely been tested empirically[10,22]. A key problem is that model predictions are of single-unit activity, but it is impossible to simultaneously measure this across the many brain regions that exhibit value-related activity. However, if such inhibitory mechanisms were to exhibit a characteristic signature that could be measured not in single cell activity, but in the summed activity of the local network, then we could use imaging techniques to search for this signature across the entire brain and isolate those regions fundamental to value comparison.

In this study, we adopted such an approach. We analysed a biophysically realistic network model of decision-making in order to generate predictions of the temporal dynamics of value correlates in local field potentials. We then applied the exact same analysis to source-reconstructed magnetoencephalography (MEG) data, a whole-brain human imaging technique that affords the requisite temporal resolution to test model predictions. Importantly, MEG allows coverage of signal from the entirety of neocortex, allowing for predictions to be tested in multiple brain regions simultaneously with high temporal resolution. Regions of ventromedial prefrontal and superior parietal cortex matched well with the biophysical model, implicating them in value comparison. Value correlates in other cortical regions matched poorly, implicating them in separate computational processes that covary with value.

Results

Biophysical model predictions

We used a mean-field version[23] of a biophysical cortical attractor network model[20] to derive predictions of the temporal dynamics of activity in a cortical region that selects between inputs reflecting the value of two options. The model comprises two populations of excitatory pyramidal cells selective for each option, with strong recurrent excitation between cells of similar selectivity, and effective inhibition between the two pools mediated by inhibitory interneurons[20] (see online methods). This effective inhibition mediates a competition between the two excitatory pools, with one pool ending up in a high firing attractor state (chosen option), and the other pool staying in a low firing attractor state (unchosen option). Neurons selective for option o receive inputs r_o at firing rates proportional to the subjective value of that option, sEV_o. The neurons further receive background noise inputs and currents from other cells in the network. Importantly, the network has very few free parameters that are not otherwise constrained by their biophysical plausibility. The behavior of single units in the network has been described elsewhere[20,24]; here, we focus on predictions suited to investigation with MEG[25], namely behavior of the summed input currents to all pyramidal cells.

We simulated network behavior using a set of trials with varying sEV_0 (as used in the human experiment, below). We sorted trials by overall value ($sEV_1 + sEV_2$; Fig. 1A top) and

value difference ($sEV_{chosen} - sEV_{unchosen}$; Fig. 1A bottom). In both cases, the network attracted faster to a decision when overall value or value difference were higher, yielding the prediction of decreased reaction times (RTs) under these conditions. We tested this prediction more formally using a multiple regression in which model RTs were predicted as a function of both overall value and value difference; both variables were found to have a negative effect on RT (fig 1B). Intuitively, the model reaches an asymmetric attractor state when the basin of attraction for this option is larger due to larger value difference (which determines the difference between the two inputs). An increase in overall value causes the network activity to rise faster and diverge faster, also resulting in faster RT.

We then performed a time-frequency analysis of network responses, which aided our subsequent comparison of model predictions with MEG data. We used Morlet wavelets to decompose network activity on each trial[26], and regressed the decomposed data onto overall value and value difference. Network transitions typically took several hundred milliseconds to occur, and so most key model predictions were limited to frequencies ranging from approximately 2–10Hz (Fig. 1C). Overall value had a broadband effect on model activity in the 3–9 Hz frequency range, soon after selective inputs were delivered to the network (Fig. 1C, top), whereas value difference had a later and slightly lower-frequency effect, predominantly in the 2–4.5 Hz range (Fig. 1C, bottom). The different frequencies reflect the fact that overall value affects the population synaptic input earlier and over a shorter time period than value difference. The effect of the two regressors on network responses is a reflection of the fact that network transitions occur at different speeds depending upon the input presented; thus, the network does not explicitly 'represent' such quantities, but these effects are a manifestation of trial-to-trial variability in the speed of the different network transitions. If we collapsed across the relevant frequencies, the temporal progression from an overall value signal to a value difference signal could be clearly seen (Fig. 1D). It was also found that on trials where the network model made an error (i.e. $sEV_{chosen} < sEV_{unchosen}$), there was an effect of overall value on the model's activity, but no clear effect of value difference (Fig. 1D, dashed lines). (However, it should be borne in mind that 'error' trials inherently covered a smaller range of value differences than 'correct' trials, which may have caused the absence of any effect). The key predictions derived from the model were therefore: (i) the temporal evolution from an 'overall' value signal to a 'difference' value signal; (ii) a difference in the frequency of the response, with value difference dominating responses at lower frequencies than overall value; (iii) the presence of an overall, but little or no difference signal, on error trials.

A distributed network of task-sensitive areas

We designed a simple value-guided choice task to test these predictions. 30 subjects repeatedly selected between two options of differing value (Fig. 2) whilst undergoing MEG. Each option had a certain number of points available, represented by the width of an onscreen bar, and a probability of obtaining those points, represented by a percentage underneath the bar. The aim was to accumulate points (displayed on a progress bar) in order to reach a gold target, at which point monetary reward was delivered and the progress bar was reset to its initial position. To accumulate maximal returns, subjects should compute the objective Pascalian value (bar width multiplied by probability of winning, denoted EV_o for option o), and select the option with the higher value on each trial. In fact, most subjects tended to overweight low probabilities of winning and underweight high probabilities, and exhibited a concave utility function, in accordance with predictions from Prospect theory (supplementary Fig. S1; supplementary table S1)[27]. Subject RTs correlated negatively with both the difference in subjective option values ($= sEV_{chosen} - sEV_{unchosen}$) and with the overall value of the decision ($= sEV_1 + sEV_2$), in line with model predictions (Fig. 1B). Fig. 3A shows a typical subject, and Fig. 3B shows the group results of a multiple linear

regression of value difference (T(29)=−7.98,p<0.0005) and overall value (T(29)= −2.36,p<0.05) on reaction times across all subjects (see also supplementary Fig. S2). We also included some trials in which both reward magnitude and probability were higher on one option than the other. There was an additional bonus in speed beyond that related to value for these 'no brainer' trials (T(29)=−8.32, p<0.0005; Fig. 3B). Subjects were therefore faster on average on these trials than on those where probability and magnitude advocated opposing choices, and so needed to be translated into a 'common currency' in which the two stimulus features could be equated. There was a steady decrease in reaction time as subjects progressed through the task (Fig. 3C), without any coincident change in parameters describing choice behavior (supplementary table S2), suggesting subjects became less deliberative and more automated in their choices as they became familiar with the task.

We used linearly constrained minimum variance beamforming[28] to spatially filter MEG data to locations in source space. We epoched data with respect to both stimulus onset and subject response, and focused our analyses on responses in the 2–10 Hz frequency range, in accordance with model predictions. We first used a whole-brain statistical parametric mapping analysis to look for areas showing a main effect of performing the task relative to a pre-stimulus (−300ms to −100ms) or post-response (+100ms to +300ms) baseline. We hypothesized that, in addition to areas important to stimulus valuation such as ventromedial prefrontal cortex, the stimulus-locked analysis would reveal early visual areas involved in basic stimulus processing, and the response-locked analysis would reveal areas involved in visually guided manual movements in parietal and premotor cortices[29], in addition to primary motor areas.

A distributed network of areas was found to be task-sensitive at these frequencies (Fig. 4A–F; supplementary movie S1, S2). Stimulus-locked, early visual cortex activation (Fig. 4A) was followed by slowly ramping bilateral activation at the frontal pole and ventromedial prefrontal cortex (Fig. 4B). Whilst 2–10Hz activity in these frontal regions peaked relatively late in the trial (1000ms after stimulus onset), it ramped from a much earlier point in the trial (see Fig. 5B and supplementary Fig. S5, discussed below). Response-locked, a prolonged activation spread from a mid-posterior portion of the superior parietal lobule, which extended medially into the marginal ramus of the posterior cingulate sulcus (Fig. 4C), to a bilateral medial portion of the mid-intraparietal sulcus (IPS) (Fig. 4D). This was followed by bilateral activation of the angular/supramarginal gyri (Fig. 4D) and right premotor cortex (Fig. 4E) before finally bilateral inferior frontal sulci and primary sensorimotor cortices (Fig. 4F) were activated at the time of the response.

Predicted network model activity in parietal and prefrontal cortex

Having isolated areas that showed changes in activity relative to baseline, we then examined whether activity within these regions co-varied with decision values, and where this activity matched with predictions derived from the biophysical decision model. Importantly, by selecting regions based on the main effect of task versus baseline, we ensured we would not be subject to a selection bias when examining these regions for value-related activity. We also investigated activity in several *a priori* defined areas commonly found to be important in functional MRI studies of decision making, bearing in mind that value correlates might not be restricted to regions showing a main effect of task versus baseline. Crucially, we applied exactly the same analysis to the timeseries from the source reconstructed MEG data as we had applied to the biophysical model (Fig. 1).

We found that activity in the right posterior superior parietal lobule (pSPL) bore several hallmarks of the biophysical model (Fig. 5A). On trials where subjects chose the option with higher subjective value ('correct' trials), activity in pSPL showed a broad correlate of overall value between 3 and 10 Hz (*p*<0.0005, permutation test, cluster corrected for

multiple comparisons across time), followed by a lower frequency (2–4Hz) correlate of value difference (Fig. 5A(ii)) ($p<0.01$, corrected), as predicted by the model (cf. Fig. 1C). When we collapsed across the relevant frequencies (Fig. 5A(iii)), activity on these correct trials differed from error trials; error trials showed a positive correlate of overall value (dashed black line, Fig. 5A(iii)) ($p<0.05$, corrected), but no such positive correlate of value difference (dashed grey line in Fig. 5A(iii); compare with Fig. 1D) ($p>0.5$). Finally, we tested an additional model prediction: that across subjects there would be a behavioral speed-accuracy tradeoff, elicited by varying the degree of recurrent excitation in the network model, and that this would predict cross-subject variance in neural data. This prediction was also found to hold in pSPL (see supplementary information; supplementary Figs. S3–4).

We also investigated whether the main effects of task performance in this region was affected by factors shown behaviorally to modulate reaction time independently of value. We looked for changes in activity in early trials relative to late trials (where reaction time was speeded, Fig. 3C), and also compared activity in trials where reward magnitude and probability advocated opposing choices with activity on 'no brainer' trials (where an additional bonus to reaction time was present beyond that explained by overall value or value difference, Fig. 3B). There was some difference between the patterns of activity in pSPL on these trials; an increase in 2–5 Hz power relative to baseline that was present on the first half of trials (Fig. 5A(i) top left) was largely absent on the second half of trials (Fig. 5A(i) bottom left). A similar distinction could be seen between activity on trials where reward magnitude and probability advocated opposing choices, and a 'common currency' representation might need to be formed (Fig. 5A(i) top right) and 'no brainer trials' (Fig. 5A(i) bottom right).

We also investigated value-related activity in ventromedial prefrontal cortex (VMPFC), focusing our analyses on a subregion that has often been shown to signal value-related metrics during decision tasks[11-16,30,31]. Notably, there has been debate over the precise role of this region in value-guided choice[6,32], perhaps triggered by the heterogeneity of responses observed there; in some functional magnetic resonance imaging (fMRI) studies it has been found to signal a difference between chosen and unchosen values[14,31], whilst in others it has appeared to signal the overall value of available reward[15], or the value of just the chosen option[16]. In VMPFC, there was an even more striking distinction between those situations where subjects would be more deliberative and exhibit slower RTs (Fig. 5B(i), top panels) versus later (Fig. 5B(i), bottom left panel) or 'no brainer' (Fig. 5B(i), bottom right panel) trials. VMPFC recruitment steadily decreased through the task, as could be seen more clearly when trials were further subdivided into separate quartiles of the experiment (supplementary Fig. S5). We found that this region transitioned from signaling overall value ($p<0.05$, corrected) to value difference ($p<0.05$, corrected) (Fig. 5B(ii)–(iii)) specifically if we restricted our analysis to the first half of trials in which it was task active (Fig. 5B(i)). When we directly contrasted the effect of overall value and value difference on early and late trials, we found that only the value difference signal was significantly stronger on earlier trials in this region (supplementary Fig. S6). There was not a significant effect of either overall value or value difference on error trials (Fig. 5B(iii), dashed lines), although the somewhat weaker signals in this region relative to pSPL may result from the relative insensitivity of MEG to deep, anterior sources, as opposed to posterior, superficial ones[33,34], and from the analysis including only half the number of trials.

One possible concern with the differences between the first and second halves of the experiment is that it might reflect more trivial cognitive differences, such as subject fatigue, rather than a change in the cortical networks underlying choice behavior. To address these concerns, we performed an additional whole-brain analysis in which we searched for regions coding more strongly for value difference in the second than in the first half of the

experiment - that is, the opposite pattern of activity witnessed in VMPFC. A bilateral portion of the anterolateral intraparietal sulcus - more lateral than the main effect pSPL activation described above - selectively reflected value difference in the second half of trials (supplementary Fig. S7). In this region, there were also no clear differences between the main effect of task performance on early versus late trials, or on harder trials versus 'no brainers' (supplementary Fig. S8).

Lastly, we also searched for effects of value in other regions identified in the main effect contrast of task vs. baseline (Fig. 4), and in several regions defined *a priori* from previous fMRI studies of value-based choice. In these analyses, we found that several areas exhibited value-dependent activity, but none of these regions matched well with predictions from the biophysical decision model (supplementary Fig. S9). We hypothesize that the value correlates in these regions might be better described by appealing to their role in other computational processes that are likely to covary with value, such as attention or response preparation. Alternatively, it may be the case that these other regions are involved in value comparison, but do so in a manner that is different to that proposed using the biophysical modeling approach.

Discussion

The cortical correlates of value during decision under risk are typically spread over a distributed network of areas, but the unique contribution of each of these areas to choice is unclear. A region involved in value comparison should receive inputs relating to the value of available options, and transform these inputs into a categorical choice. We used a biophysically plausible model that exhibits this property to derive novel predictions of the temporal dynamics of cortical activity. We applied linear regression to investigate at which timepoints and in which frequency bands value correlates could be found in network activity. These responses typically occurred in low frequencies (<10 Hz), consistent with a slow integrative process. We then applied the same analysis to source-reconstructed MEG data, in order to identify regions involved in value comparison. A distributed network of areas were task-sensitive at the relevant frequencies, but only pSPL and VMPFC closely matched predictions of the biophysical model, with the latter doing so selectively in trials early in the experiment. Other regions were found to show value correlates, but did not match closely with predictions from the biophysical model; this suggests that extensions to the model are necessary to fully capture the role of different brain regions in the task. Furthermore, MEG will be limited in its ability to resolve sources from deep brain structures that do not possess an 'open field' layout, such as in striatum[17]; thus, the role of alternative mechanisms for selection (dependent upon cortico-basal ganglia loops) cannot be addressed in the current study.

A key feature of the biophysical model is the ability to slowly integrate value-related inputs, afforded by its recurrent excitatory structure and long synaptic time constants mediated by NMDA receptors. It is not immediately obvious that value comparison should be subject to a process of integration in the same way as a noisy sensory stimulus. However, the observed distribution of reaction times fits well with a process of integration, as has been investigated more closely in previous studies that used a 'drift diffusion' model to predict reaction times[35,36]. The drift diffusion model was originally designed to make predictions of behavioral data, and has often been used to make predictions of single unit activity during perceptual choice. However, because it essentially describes differences in activity between different populations of selective cells and also ignores any non-selective activity, it is not transparent how to make predictions of imaging measures such as MEG or fMRI. In this study, we elected to use a biophysical implementation of a competition model, which makes clear and explicit predictions of the measurable data. Unsurprisingly, when we used the

pseudo-variable in the DDM as a marker for integrated brain activity, we found differences between the predictions (supplementary information; supplementary Fig. S10).

The predictions from the model also form a striking example of the distinction between two types of representation - 'content' and 'functional' representations - in cortical circuits[37]. To the external observer, recording with an imaging technique (or an electrode), the content of the network first appears to 'represent' the overall value and later the value difference between the two options. By contrast, the *functional* representations in the network - those used by the brain - are quite different. There is a representation of option values on the input to the network, and a representation of choice on the outputs of the network, as should be decoded by a suitable downstream observer. The reason that the network shows value-related activity is simply that the same network transitions occur faster on high value and high value difference trials. Hence, whilst neural activity in the network may covary with the overall value and value difference, this content need never be decoded by another brain region. Thus, the extent to which the network can be said to functionally 'represent' these two quantities in a meaningful way is questionable[37].

The region in pSPL isolated as matching with model predictions is close to the cytoarchitectonic region hIP3[38], which may be the human homologue of the medial intraparietal area (MIP). It is also referred to as IPS4 and DIPSA, which resembles macaque MIP[39]. In the macaque, this region is often implicated in visually-guided movements of the forelimbs[29]. It may therefore have a role in integrating information in order to guide limb movements that is analogous to the role of LIP in generating saccades. This process of saccade generation is closely linked to the tracking of value associated with generating a saccade in a particular direction[9,10].

The region in VMPFC is often found using fMRI to be responsive to the value of stimuli during decision tasks[11-16,30,31], but its precise role has been debated[6,32], perhaps as a result of the relative absence of published single-unit recording data in comparison to the nearby lateral orbitofrontal cortex[5,7]. In early trials, this region was found to transition from signaling overall value to signaling value difference. Strikingly, this same transition was also recently found in single-unit recordings from the most ventral portion of the striatum[17], which receives a particularly dense projection from VMPFC[40], and also in prefrontal cortex[41]. Similarly to the present study, this task required monkeys to combine two stimulus properties to form their decision, namely the reward magnitude and the delay to reward delivery. In our task, VMPFC was selectively activated in trials where subjects had to combine probability and magnitude information to choose accurately. This is also consistent with the finding that lesions to this area, but not nearby lateral orbitofrontal cortex, produce impairments in value comparison[32], and more specifically produce changes in tasks where multiple dimensions have to be considered in forming a choice[42].

Some previous studies have attempted to apply a modeling approach to capture signals from distributed cortical regions during choice, measured using fMRI. These studies have made predictions based either on drift diffusion models[43] or biophysically plausible networks[44] but the predictions of these models are heavily dependent upon whether fMRI signal is assumed to reflect activity from all timepoints including after a decision has been formed[44], or whether it only reflects activity until the decision threshold is reached[43]. Moreover, several key predictions of these models also relate to how their activity evolves over time as a decision is made, and the slow hemodynamic response means fMRI is limited in how well it can tease apart these predictions of temporal dynamics. We argue that it is important to use a time-resolved technique, such as MEG, to test these predictions.

Biophysically-inspired models have also been used to infer the structure of connections between or within different cortical areas from M/EEG data[45]. However, these studies have not inferred the specific neuronal mechanism underlying a particular cognitive process, as we have proposed here. The present model performs the critical *computation* of transforming value-related inputs into a choice, and does so in a way that has captured single-unit activity during perceptual decision tasks. The application of this computational biophysical modeling approach may not be limited to decision making paradigms. Novel predictions might, for instance, be derived from biophysical models already designed to capture single unit data in inhibitory control or working memory processes[46]. In models of working memory, for instance, gamma-band (30–70 Hz) responses can be elicited[46], and parametric modulation of input to these models may explain variation in gamma-band frequencies seen during working memory tasks in frontal cortex[47]. Alternatively, by varying internal parameters of a biophysical model, novel predictions might be derived of the effects of cross-subject variation on cortical responses measurable with M/EEG (see also supplementary discussion). Because these parameters relate to specific biophysical properties such as the density of network connectivity or the concentration of a specific neurotransmitter, it may be possible to directly relate these parameters to cross-subject variation in these properties, for instance via local measurements of neurotransmitter concentrations[48], or perhaps genetic polymorphism or pharmacological challenge.

Supplementary Material

Refer to Web version on PubMed Central for supplementary material.

Acknowledgments

References

1. von Neumann, J.; Morgenstern, O. Theory of games and economic behavior. Princeton University Press; 1944.

2. Dickinson A, Balleine B. Motivational control of goal-directed action. Animal Learning and Behavior. 1994; 22:1–18.

3. Stephens, DW.; Krebs, JR. Foraging theory. Princeton University Press; 1986.

4. Sutton, R.; Barto, A. Reinforcement learning: an introduction. MIT Press; 1998.

5. Rushworth MSF, Behrens TEJ. Choice, uncertainty and value in prefrontal and cingulate cortex. Nat Neurosci. 2008; 11:389–397. doi:10.1038/nn2066. [PubMed: 18368045]

6. Kable JW, Glimcher PW. The neurobiology of decision: consensus and controversy. Neuron. 2009; 63:733–745. doi:10.1016/j.neuron.2009.09.003. [PubMed: 19778504]

7. Padoa-Schioppa C. Neurobiology of Economic Choice: A Good-Based Model. Annu Rev Neurosci. 2011; 34:333–359. doi:10.1146/annurev-neuro-061010-113648. [PubMed: 21456961]

8. Rangel A, Camerer CF, Montague PR. A framework for studying the neurobiology of value-based decision making. Nature Reviews Neuroscience. 2008; 9:545–556. doi:10.1038/nrn2357.

9. Platt ML, Glimcher PW. Neural correlates of decision variables in parietal cortex. Nature. 1999; 400:233–238. doi:10.1038/22268. [PubMed: 10421364]

10. Sugrue LP, Corrado GS, Newsome WT. Matching behavior and the representation of value in the parietal cortex. Science. 2004; 304:1782–1787. doi:10.1126/science.1094765. [PubMed: 15205529]

11. Tom SM, Fox CR, Trepel C, Poldrack RA. The neural basis of loss aversion in decision-making under risk. Science. 2007; 315:515–518. doi:10.1126/science.1134239. [PubMed: 17255512]

12. Plassmann H, O'Doherty JP, Rangel A. Orbitofrontal cortex encodes willingness to pay in everyday economic transactions. J Neurosci. 2007; 27:9984–9988. doi:10.1523/JNEUROSCI. 2131-07.2007. [PubMed: 17855612]

13. Knutson B, Taylor J, Kaufman M, Peterson R, Glover G. Distributed neural representation of expected value. J Neurosci. 2005; 25:4806–4812. doi:10.1523/JNEUROSCI.0642-05.2005. [PubMed: 15888656]

14. Boorman ED, Behrens TEJ, Woolrich MW, Rushworth MSF. How green is the grass on the other side? Frontopolar cortex and the evidence in favor of alternative courses of action. Neuron. 2009; 62:733–743. doi:10.1016/j.neuron.2009.05.014. [PubMed: 19524531]

15. Blair K, et al. Choosing the lesser of two evils, the better of two goods: specifying the roles of ventromedial prefrontal cortex and dorsal anterior cingulate in object choice. J Neurosci. 2006; 26:11379–11386. doi:26/44/11379 [pii] 10.1523/JNEUROSCI.1640-06.2006. [PubMed: 17079666]

16. Kable JW, Glimcher PW. The neural correlates of subjective value during intertemporal choice. Nat Neurosci. 2007; 10:1625–1633. doi:10.1038/nn2007. [PubMed: 17982449]

17. Cai X, Kim S, Lee D. Heterogeneous Coding of Temporally Discounted Values in the Dorsal and Ventral Striatum during Intertemporal Choice. Neuron. 2011; 69:170–182. doi:S0896-6273(10)00983-9 [pii] 10.1016/j.neuron.2010.11.041. [PubMed: 21220107]

18. Kennerley SW, Dahmubed AF, Lara AH, Wallis JD. Neurons in the frontal lobe encode the value of multiple decision variables. Journal of Cognitive Neuroscience. 2009; 21:1162–1178. doi: 10.1162/jocn.2009.21100. [PubMed: 18752411]

19. Usher M, McClelland JL. The time course of perceptual choice: the leaky, competing accumulator model. Psychological review. 2001; 108:550–592. [PubMed: 11488378]

20. Wang XJ. Probabilistic decision making by slow reverberation in cortical circuits. Neuron. 2002; 36:955–968. [PubMed: 12467598]

21. Shadlen MN, Newsome WT. Neural basis of a perceptual decision in the parietal cortex (area LIP) of the rhesus monkey. J Neurophysiol. 2001; 86:1916–1936. [PubMed: 11600651]

22. Soltani A, Wang XJ. A biophysically based neural model of matching law behavior: melioration by stochastic synapses. J Neurosci. 2006; 26:3731–3744. doi:26/14/3731 [pii] 10.1523/JNEUROSCI. 5159-05.2006. [PubMed: 16597727]

23. Wong KF, Huk AC, Shadlen MN, Wang XJ. Neural circuit dynamics underlying accumulation of time-varying evidence during perceptual decision making. Front Comput Neurosci. 2007; 1:6. doi: 10.3389/neuro.10.006.2007. [PubMed: 18946528]

24. Wong KF, Wang XJ. A recurrent network mechanism of time integration in perceptual decisions. J Neurosci. 2006; 26:1314–1328. doi:10.1523/JNEUROSCI.3733-05.2006. [PubMed: 16436619]

25. Hämäläinen MS, Hari R, Ilmoniemi RJ, Knuutila J. Magnetoencephalography—theory, instrumentation, and applications to noninvasive studies of the human brain. Reviews of Modern Physics. 1993; 65:413–497.

26. Tallon-Baudry C, Bertrand O, Delpuech C, Permier J. Oscillatory gamma-band (30-70 Hz) activity induced by a visual search task in humans. J Neurosci. 1997; 17:722–734. [PubMed: 8987794]

27. Tversky A, Kahneman D. Advances in prospect theory: cumulative representation of uncertainty. J Risk Uncert. 1992; 5:297–323.

28. VanVeen BD, vanDrongelen W, Yuchtman M, Suzuki A. Localization of brain electrical activity via linearly constrained minimum variance spatial filtering. Ieee Transactions on Biomedical Engineering. 1997; 44:867–880. [PubMed: 9282479]

29. Johnson PB, Ferraina S, Bianchi L, Caminiti R. Cortical networks for visual reaching: physiological and anatomical organization of frontal and parietal lobe arm regions. Cereb Cortex. 1996; 6:102–119. [PubMed: 8670643]

30. Gershman SJ, Pesaran B, Daw ND. Human reinforcement learning subdivides structured action spaces by learning effector-specific values. J Neurosci. 2009; 29:13524–13531. doi:10.1523/JNEUROSCI.2469-09.2009. [PubMed: 19864565]

31. Serences JT. Value-based modulations in human visual cortex. Neuron. 2008; 60:1169–1181. doi:10.1016/j.neuron.2008.10.051. [PubMed: 19109919]

32. Noonan MP, et al. Separate value comparison and learning mechanisms in macaque medial and lateral orbitofrontal cortex. Proc Natl Acad Sci U S A. 2010; 107:20547–20552. doi:1012246107 [pii] 10.1073/pnas.1012246107. [PubMed: 21059901]

33. Hillebrand A, Barnes GR. A quantitative assessment of the sensitivity of whole-head MEG to activity in the adult human cortex. Neuroimage. 2002; 16:638–650. doi:S105381190291102X [pii]. [PubMed: 12169249]

34. Marinkovic K, Cox B, Reid K, Halgren E. Head position in the MEG helmet affects the sensitivity to anterior sources. Neurol Clin Neurophysiol. 2004; 2004:30. doi:30 [pii]. [PubMed: 16012659]

35. Sigman M, Dehaene S. Parsing a cognitive task: a characterization of the mind's bottleneck. PLoS Biol. 2005; 3:e37. doi:10.1371/journal.pbio.0030037. [PubMed: 15719056]

36. Milosavljevic M, Malmaud J, Huth A, Koch C, Rangel A. The drift diffusion model can account for the accuracy and reaction time of value-based choices under high and low time pressure. Judgement and decision making. 2010; 5:437–449.

37. deCharms RC, Zador A. Neural representation and the cortical code. Annu Rev Neurosci. 2000; 23:613–647. doi:10.1146/annurev.neuro.23.1.613. [PubMed: 10845077]

38. Scheperjans F, et al. Observer-independent cytoarchitectonic mapping of the human superior parietal cortex. Cereb Cortex. 2008; 18:846–867. doi:bhm116 [pii] 10.1093/cercor/bhm116. [PubMed: 17644831]

39. Mars RB, et al. Diffusion weighted imaging tractography-based parcellation of the human parietal cortex and comparison with human and macaque resting state functional connectivity. J Neurosci. 2011; 31:4087–4100. [PubMed: 21411650]

40. Haber SN, Kim KS, Mailly P, Calzavara R. Reward-related cortical inputs define a large striatal region in primates that interface with associative cortical connections, providing a substrate for incentive-based learning. J Neurosci. 2006; 26:8368–8376. doi:26/32/8368 [pii] 10.1523/JNEUROSCI.0271-06.2006. [PubMed: 16899732]

41. Kim S, Lee D. Prefrontal cortex and impulsive decision making. Biol Psychiatry. 2011; 69:1140–1146. doi:S0006-3223(10)00711-0 [pii] 10.1016/j.biopsych.2010.07.005. [PubMed: 20728878]

42. Fellows LK. Deciding how to decide: ventromedial frontal lobe damage affects information acquisition in multi-attribute decision making. Brain. 2006; 129:944–952. doi:awl017 [pii] 10.1093/brain/awl017. [PubMed: 16455794]

43. Basten U, Biele G, Heekeren HR, Fiebach CJ. How the brain integrates costs and benefits during decision making. Proc Natl Acad Sci U S A. 2010; 107:21767–21772. doi:0908104107 [pii] 10.1073/pnas.0908104107. [PubMed: 21118983]

44. Rolls ET, Grabenhorst F, Deco G. Choice, difficulty, and confidence in the brain. Neuroimage. 2010; 53:694–706. doi:S1053-8119(10)00950-X [pii] 10.1016/j.neuroimage.2010.06.073. [PubMed: 20615471]

45. Kiebel SJ, Garrido MI, Moran R, Chen CC, Friston KJ. Dynamic causal modeling for EEG and MEG. Human Brain Mapping. 2009; 30:1866–1876. doi:10.1002/hbm.20775. [PubMed: 19360734]

46. Compte A, Brunel N, Goldman-Rakic PS, Wang XJ. Synaptic mechanisms and network dynamics underlying spatial working memory in a cortical network model. Cereb Cortex. 2000; 10:910–923. [PubMed: 10982751]

47. Meltzer JA, et al. Effects of working memory load on oscillatory power in human intracranial EEG. Cereb Cortex. 2008; 18:1843–1855. doi:bhm213 [pii] 10.1093/cercor/bhm213. [PubMed: 18056698]

48. Muthukumaraswamy SD, Edden RA, Jones DK, Swettenham JB, Singh KD. Resting GABA concentration predicts peak gamma frequency and fMRI amplitude in response to visual stimulation in humans. Proc Natl Acad Sci U S A. 2009; 106:8356–8361. doi:0900728106 [pii] 10.1073/pnas.0900728106. [PubMed: 19416820]

49. Hsu M, Krajbich I, Zhao C, Camerer CF. Neural Response to Reward Anticipation under Risk Is Nonlinear in Probabilities. J Neurosci. 2009; 29:2231–2237. doi:10.1523/JNEUROSCI. 5296-08.2009. [PubMed: 19228976]

50. Berg P, Scherg M. A multiple source approach to the correction of eye artifacts. Electroencephalogr Clin Neurophysiol. 1994; 90:229–241. [PubMed: 7511504]
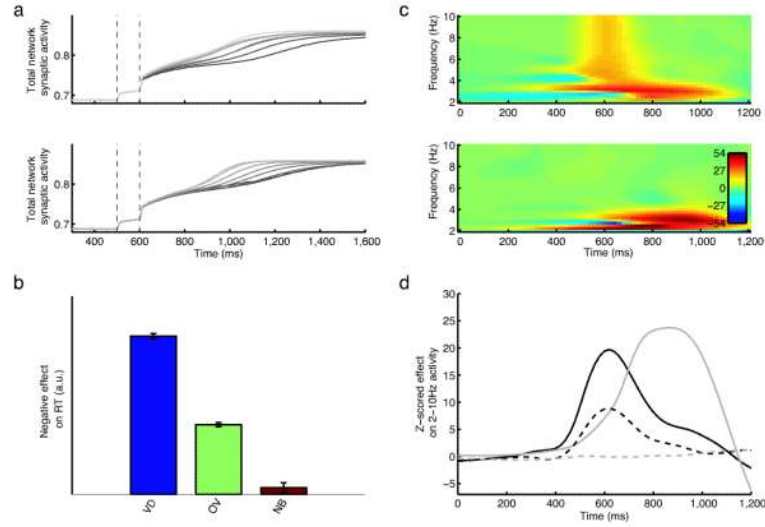
Figure 1. Predictions of neural activity from cortical attractor network model
(A) Top panel: summed network postsynaptic currents as a function of time through trial, sorted and binned into trials with high overall value (lighter shades of grey) through trials with low overall value (dark grey/black). Bottom panel: As top panel, resorted and binned by value difference between chosen and unchosen options. (B) Effect of value difference (VD), overall value (OV) and 'no brainer' (NB) trials on reaction time, estimated using multiple regression (mean +/− s.e. of effect size; Y-axis is flipped, so positive values equate to a negative effect on reaction times). (C) Time-frequency spectra of effects of overall value (top panel) and value difference (bottom panel) on network model activity, estimated with multiple regression. Color indicates Z-statistic. (D) Z-scored effect of overall value (on frequency range 3–9Hz; black lines) and value difference (on frequency range 2–4.5 Hz; grey lines); solid lines are correct trials, dashed lines incorrect trials.
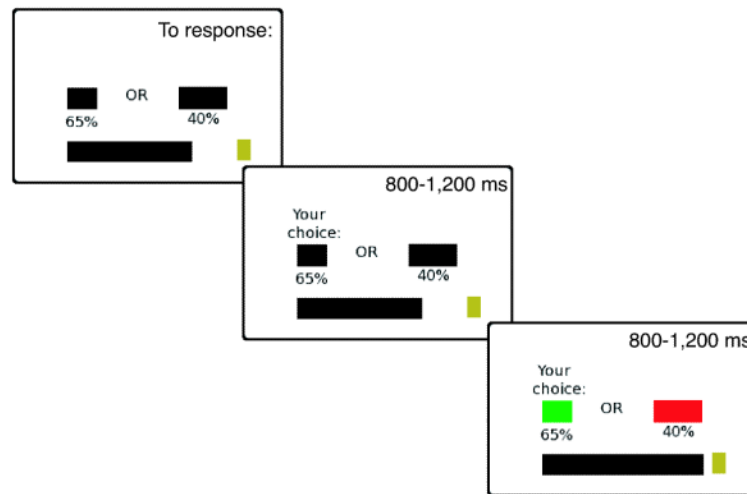
Figure 2. Value-based decision task

Task schematic. Subjects repeatedly chose between two risky prospects to obtain monetary reward. Stimuli comprised a rectangular bar, whose width determined the amount of reward available, and a number presented underneath the bar, whose value determined the probability of receiving reward on that option. Stimuli were drawn such that reward magnitude/probability were never identical across the two options; subjects therefore needed to integrate across stimulus dimensions to make optimal choices. On some trials, however, both probability and magnitude were larger on one side than the other – a 'no brainer' trial. Subjects had unlimited time to respond, and received feedback on both chosen and unchosen options – green for rewarded option, red for non-rewarded.
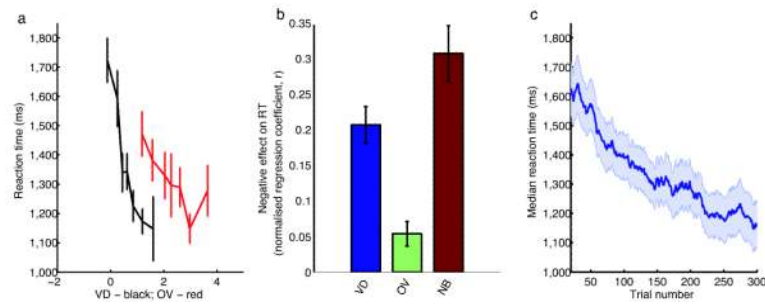
Figure 3. Subject behavior

(A) Reaction time (mean +/− s.e.) for an example subject, as a function of subjective value difference (black) and subjective overall value (red). (B) Effects of value difference (VD), overall value (OV) and 'no brainer trials' (NB) on subject reaction times (mean +/− s.e. across subjects), estimated using linear regression. Y-axis is flipped; positive values equate to a negative effect on reaction times. (C) Running group mean +/− s.e. of reaction time (smoothed across 40 trials) as a function of trial number. See also supplementary figures S1/ S2.
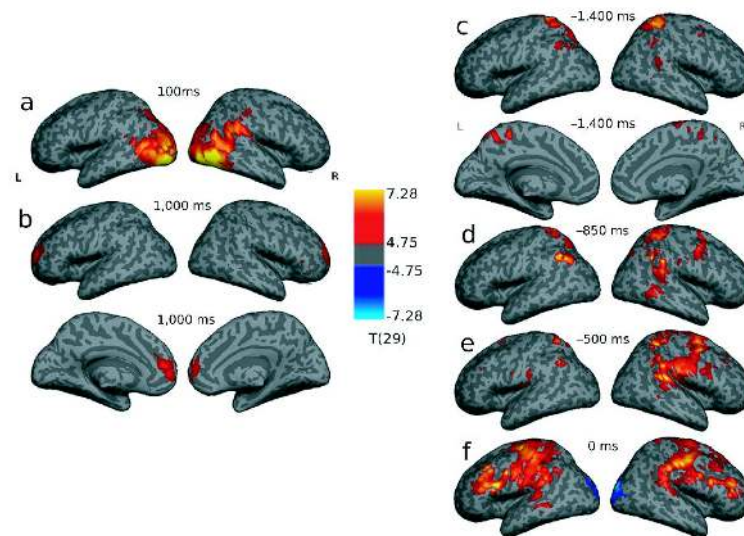
Figure 4. Main effect of task performance on activity in 2–10Hz frequency range
(A)/(B) Stimulus locked activity. Group T-map of effect of task performance relative to a −300 to −100 ms (pre-stimulus) baseline; (A) 100ms post-stimulus, early visual activation (peak T(29)=10.00, 100ms, MNI (40,−74,6)); (B) 1000ms post-stimulus, activation at frontal pole (T(29)=7.23, 1125ms, MNI (22,58,26) and ventromedial prefrontal cortex (T(29)=5.20, 1000ms, MNI (43,60,35)). (C)–(F) Response locked activity. Effect of task performance relative to a +100ms to +300ms (post-response) baseline; (C) 1400ms pre-response, activation at pSPL/posterior cingulate (T(29)=7.05, −1625ms (pre-response), MNI(18,−44,62) and mid-IPS (T(29)=8.20, −525ms, MNI(30,−46,56) (right) and T(29)=7.55,−700ms, MNI (−24,−42,74) (left)); (D) 850ms pre-response, activation at angular/supramarginal gyri (T(29)=8.46, −725ms, MNI (56,−50,40) (right) and T(29)=8.69, −725ms, MNI (−50,−60,42) (left)); (E) 500ms pre-response, premotor activation (T(29)=7.35,−450 ms, MNI (38,−2,64); (F) time of response, activation at inferior frontal sulci (T(29)=8.02, 0ms, MNI (−54, 12, 28) (left) and T(29)=7.55, −75ms, MNI (48,10,30) (right)) and sensorimotor cortices (T(29)=7.57, −75ms, MNI (−50,−28,58) (left) and T(29)=8.02, 0ms, MNI (−54,12,28) (right). All images are thresholded at T>4.75 ($p<5*10^{-5}$ uncorrected) for display purposes. See also supplementary movies S1 and S2.
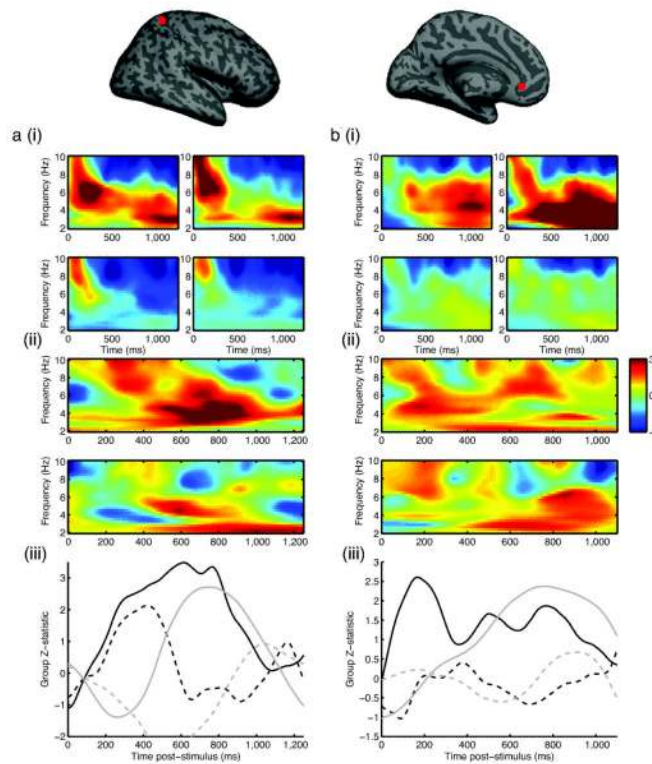
Figure 5. pSPL (MNI 18, −44, 62mm) and VMPFC (MNI 6, 28, −8 mm) shows several value-related hallmarks of the biophysical network model

(A)(i) pSPL: Main effect of task performance relative to pre-stimulus baseline on first half of trials (top left panel) and second half of trials (bottom left panel); main effect of task performance on trials where reward magnitude and probability advocate opposing choices (top right panel), and 'no brainer' trials (bottom right panel). Color indicates group Z-statistic. (ii) Time-frequency spectra of effects of overall value (top panel) and value difference (bottom panel) on activity in pSPL, estimated using multiple regression. Analysis is equivalent to that performed in figure 1C on biophysical model. Color indicates group Z-statistic. (iii) Effect of overall value (3–9Hz, black) and value difference (2–4.5 Hz, grey) on correct/error trials (solid/dashed lines respectively). (B)(i) Main effect of task in VMPFC, sorted as in figure 5A(i). (ii) VMPFC effects of overall value and value difference, as for pSPL, but restricted to first half of experiment. (iii) VMPFC collapsed value effects, as for pSPL, but restricted to first half of experiment.